ELSEVIER

Journal of Chromatography A, 862 (1999) 1–16

JOURNAL OF CHROMATOGRAPHY A

www.elsevier.com/locate/chroma

Calculation of chromatographic band profiles with an implicit isotherm

Krzysztof Kaczmarski*, Dorota Antos

Faculty of Chemistry, Chemical Engineering Department, Rzeszów University of Technology, Al. Powstańców Warszawy 6, 35-959 Rzeszów, Poland

Received 4 June 1999; received in revised form 4 August 1999; accepted 17 August 1999

Abstract

The numerical method for solving the mathematical model of chromatography process coupled with implicit isotherm has been proposed. The exemplary predictions of elution band profiles were performed for competitive adsorption data of 2-phenylethanol and 3-phenylpropanol on ODS-silica with methanol–water as the mobile phase. The simulations of chromatography process with various isotherm models taking into account lateral interactions in adsorbed phase and surface heterogeneity were discussed.

Keywords: Implicit isotherms; Equilibrium-dispersive model; Reaction-dispersive model; Band profiles; Adsorption isotherms; 2-Phenylethanol; 3-Phenylpropanol

1. Introduction

Determination of an isotherm equation that describes the distribution between mobile and stationary phase has fundamental importance in the studies of adsorption-based separation process. Mathematical adsorption models based on mass balance equations of compounds separated, coupled with isotherm equations, permit one to simulate the adsorption process. The adequate isotherm model allows the possibility of accurate prediction of elution band profiles under various operating conditions and allows optimisation of the separation process.

A number of isotherm models are used to correlate the single-component and competitive adsorption data. Some of them, like the Langmuir isotherm, assume an ideal system behaviour and in some cases, especially of multicomponent systems in strongly overloaded preparative chromatography, are unable to properly predict the separation process. Other models, like the Fowler–Guggenheim [1], take into account the possibility of adsorbate–adsorbate interactions in adsorbed phase or surface heterogeneity as the bi-Langmuir, Freundlich and the more complex – Jovanovic–Freundlich [2]. The most sophisticated isotherms account for lateral interactions and surface heterogeneity – Fowler–Guggenheim/Langmuir–Freundlich, Fowler–Guggenheim/Jovanovic–Freundlich [3,4]. As evidenced in Ref. [4] the multicomponent isotherms considering both lateral interactions and surface heterogeneity better describe competitive adsorption data. Additionally, these models are purely predictive – and are based solely on single component parameters. The parameters of isotherm equations are determined by fitting the model to the

*Corresponding author.
E-mail address: ichkk@ewa.prz.rzeszow.pl (K. Kaczmarski)

0021-9673/99/$ – see front matter
PII: S0021-9673(99)00901-2

experimental adsorption data of single components.

The isotherm equations mentioned above include complex implicit functions of the adsorbed phase concentration. Their application for simulation of band profiles was practically impossible until now because, as was stated in Refs. [4–6], numerical inversion of implicit isotherm prohibitively increases the calculation time. In this paper we propose the numerical method for solving the chromatography column model with an isotherm accounting for lateral interaction and surface heterogeneity in reasonable computational time.

2. Theory

2.1. Isotherm models

The numerical method described in next section was used for simulations of the elution band profiles of 2-phenylethanol and 3-phenylpropanol on ODS-silica with methanol–water as the mobile phase. Competitive adsorption data were reported in Ref. [5] and tested for various isotherm models in Refs. [4,7]. On the basis of regression analysis of adsorption data reported in Ref. [4] we decided to examine the isotherm equations that exhibited the highest value of the Fisher parameter [4]:

$$F_{\mathrm{calc}} = \frac{(n-l)\sum_{i=1}^{n}(\mathrm{q}_{\mathrm{exp},i} - \overline{\mathrm{q}_{\mathrm{exp}}})^2}{(n-1)\sum_{i=1}^{n}(\mathrm{q}_{\mathrm{exp},i} - \mathrm{q}_{\mathrm{calc},i})^2}$$

where $\mathbf{q}_{\mathrm{exp},i}$ represents the vector of experimental adsorbed phase concentration, $\mathbf{q}_{\mathrm{calc},i}$, the vector predicted by model, $\overline{\mathbf{q}_{\mathrm{exp},i}}$, the mean value of vector $\mathbf{q}_{\mathrm{exp},i}$, n, the number of data points, l, the number of adjusted parameters. Since the denominator contains residual sum of squares, the higher the value of the Fisher parameter the better the experimental data are correlated.

The highest F_{calc} values were achieved for the most complex isotherms that take into account both lateral interaction in adsorbed phase and heterogeneity of surface: Fowler–Guggenheim/Langmuir–Freundlich (FG/LF) and Fowler–Guggenheim/Jovanovic–Freundlich (FG/JF) [4].

The competitive isotherm model FG/LF is expressed by following set of equations:

$$\theta_1 = a_1 C_1 e^{\chi_1\theta_1 + \chi_{12}\theta_2} \times \frac{\left[a_1 C_1 e^{\chi_1\theta_1 + \chi_{12}\theta_2} + a_2 C_2 e^{\chi_{21}\theta_1 + \chi_2\theta_2}\right]^{\nu_1 - 1}}{\left\{1 + \left[a_1 C_1 e^{\chi_1\theta_1 + \chi_{12}\theta_2} + a_2 C_2 e^{\chi_{21}\theta_1 + \chi_2\theta_2}\right]^{\nu_1}\right\}} \quad (1)$$

$$\theta_2 = a_2 C_2 e^{\chi_{21}\theta_1 + \chi_2\theta_2} \times \frac{\left[a_1 C_1 e^{\chi_1\theta_1 + \chi_{12}\theta_2} + a_2 C_2 e^{\chi_{21}\theta_1 + \chi_2\theta_2}\right]^{\nu_2 - 1}}{\left\{1 + \left[a_1 C_1 e^{\chi_1\theta_1 + \chi_{12}\theta_2} + a_2 C_2 e^{\chi_{21}\theta_1 + \chi_2\theta_2}\right]^{\nu_2}\right\}} \quad (2)$$

where ν is the heterogeneity parameter (with $0 < \nu < 1$). The parameters χ_1 and χ_2 relate to the energy of lateral interaction between molecules of corresponding components. Parameters χ_{21} and χ_{12} account for the cross interaction between separated components. θ_i is fractional coverage of ith component: $\theta_i = q_i/q_{is}$, q_{is} is the total coverage, C_i, the component concentration in the bulk phase.

The competitive FG/JF model consists of equations:

$$\theta_1 = \Phi_1\left\{1 - e^{-\left[a_1 C_1 e^{\chi_1\theta_1 + \chi_{12}\theta_2} + a_2 C_2 e^{\chi_{21}\theta_1 + \chi_2\theta_2}\right]^{\nu_1}}\right\} \quad (3)$$

$$\theta_2 = \Phi_2\left\{1 - e^{-\left[a_1 C_1 e^{\chi_1\theta_1 + \chi_{12}\theta_2} + a_2 C_2 e^{\chi_{21}\theta_1 + \chi_2\theta_2}\right]^{\nu_2}}\right\} \quad (4)$$

where:

$$\Phi_1 = \frac{a_1 C_1 e^{\chi_1\theta_1 + \chi_{12}\theta_2}}{a_1 C_1 e^{\chi_1\theta_1 + \chi_{12}\theta_2} + a_2 C_2 e^{\chi_{21}\theta_1 + \chi_2\theta_2}}$$

$$\Phi_2 = \frac{a_2 C_2 e^{\chi_{21}\theta_1 + \chi_2\theta_2}}{a_1 C_1 e^{\chi_1\theta_1 + \chi_{12}\theta_2} + a_2 C_2 e^{\chi_{21}\theta_1 + \chi_2\theta_2}}$$

Ignoring the lateral interaction in Eqs. (3) and (4) one can obtain the Jovanovic–Freundlich (JF) model:

$$\theta_1 = \frac{a_1 C_1}{a_1 C_1 + a_2 C_2}\left[1 - e^{-(a_1 C_1 + a_2 C_2)^{\nu_1}}\right] \quad (5)$$

$$\theta_2 = \frac{a_2 C_2}{a_1 C_1 + a_2 C_2}\left[1 - e^{-(a_1 C_1 + a_2 C_2)^{\nu_2}}\right] \quad (6)$$

Similarly, neglecting surface heterogeneity in Eqs.

(1) and (2) the Fowler–Guggenheim (FG) model can be derived:

$$K_1 C_1 = \frac{\theta_1}{1-\theta_1-\theta_2} e^{-(\chi_1\theta_1+\chi_{12}\theta_2)} \quad (7)$$

$$K_2 C_2 = \frac{\theta_2}{1-\theta_1-\theta_2} e^{-(\chi_{21}\theta_1+\chi_2\theta_2)} \quad (8)$$

All the aforementioned models were solved with numerical methods discussed below. The isotherm parameters presented in Table 1 were applied as in Ref. [4].

Table 1
Results of regression analysis [4]

Model	Parameter	F_{calc}
Model FG/FL	$q_{s1}=59$	136.26
Eqs. (1) and (2)	$a_1=0.03696$	
	$\chi_1=0.9126$	
	$\nu_1=0.9865$	
	$q_{s2}=112$	
	$a_2=0.02424$	
	$\chi_2=1.4174$	
	$\nu_2=0.8251$	
Model FG/JF	$q_{s1}=42$	134.66
Eqs. (3) and (4)	$a_1=0.05292$	
	$\chi_1=0.4122$	
	$\nu_1=0.988$	
	$q_{s2}=83$	
	$a_2=0.03591$	
	$\chi_2=0.6672$	
	$\nu_2=0.832$	
Model JF	$q_{s1}=74$	85.53
Eqs. (5) and (6)	$a_1=0.029$	
	$\nu_1=1.0$	
	$q_{s2}=126$	
	$a_2=0.02781$	
	$\nu_2=0.891$	
Model FG	$q_{s1}=75$	69.2
Eqs. (7) and (8)	$K_1=0.03047$	
	$\chi_1=0.6434$	
	$q_{s2}=316$	
	$K_2=0.0153$	
	$\chi_2=-2.037$	
Competitive Langmuir	$q_{s1}=154$	22.99
	$K_1=0.015$	
	$q_{s2}=134$	
	$K_2=0.035$	

2.2. Method of calculation

For simulation of chromatography column dynamic the following model was used:

$$\frac{\partial C_i}{\partial t} + \frac{1-\epsilon_t}{\epsilon_t}\frac{\partial q_i}{\partial t} + \frac{u}{\epsilon_t}\frac{\partial C_i}{\partial x} = D_a \frac{\partial^2 C_i}{\partial x^2} \quad (9)$$

where: t is the time, ϵ_t, the total porosity, u, the superficial velocity, x, the axial coordinate, D_a, the apparent dispersion coefficient calculated from the equation $D_a = u^*L/(2^*N^*\epsilon_t)$, N, the number of theoretical plates, L, the column length, $i=1,..,NC$, and NC, the number of components.

Eq. (9) was solved using two methods: (a) orthogonal collocation on finite element (OCFE), (b) finite difference (FD) with typical initial conditions:

$$\text{for } t=0;\ 0<x<L,\ C_i=0,\ q_i=0 \quad (10)$$

In the case of the OCFE method, Danckwerts boundary conditions were used: for $t>0$; $x=0$:

$$u^*C'_{fi} - u^*C_i(0) = -D_a\frac{\partial C_i}{\partial x};\ C'_{fi} = \begin{cases} C_{fi} & \text{for } t\in(0,t_p) \\ 0 & \text{for } t>t_p \end{cases} \quad (11)$$

for $t>0$; $x=L$:

$$\frac{\partial C_i}{\partial x} = 0 \quad (12)$$

where C_{fi} denotes the inlet concentration of component number i, t_p is time during the constant concentration C_f is fed into the column.

In the high-performance liquid chromatography (HPLC) column case Danckwerts conditions (Eq. (11)) are often replaced with the simpler:

$$C_i(0) = C'_{fi};\ C'_{fi} = \begin{cases} C_{fi} & \text{for } t\in(0,t_p) \\ 0 & \text{for } t>t_p \end{cases} \quad (11a)$$

Eq. (11a) was applied in this work for solving mass balance (Eq. (9)) with the FD method.

If the rate of adsorption–desorption process is assumed infinitely fast, Eq. (9) is coupled with the appropriate isotherm equation:

$$q_i = f(\mathbf{C}) \quad (13)$$

or for the implicit equation:

$$f(\mathbf{C},\mathbf{q}) = 0 \quad (13a)$$

where **C** and **q** are vectors of concentration of the components in bulk and stationary phases, respectively.

The set of Eqs. (9) and (13) is known as the equilibrium-dispersive model.

Differential mass balance (Eq. (9)) can be rewritten to more convenient for the solution form. Taking into account that the time derivative $\partial q_i/\partial t$ is equal to:

$$\frac{\partial q_i}{\partial t} = \sum_{m=1}^{\mathrm{NC}} \frac{\partial q_i}{\partial C_m}\frac{\partial C_m}{\partial t} \tag{14}$$

Eq. (9) can be expressed as follows:

$$\frac{\partial C_i}{\partial t} + \frac{1-\epsilon_t}{\epsilon_t}\sum_{m=1}^{\mathrm{NC}} \frac{\partial q_i}{\partial C_m}\frac{\partial C_m}{\partial t} + \frac{u}{\epsilon_t}\frac{\partial C_i}{\partial x} = D_a\frac{\partial^2 C_i}{\partial x^2} \tag{15}$$

When the kinetics of the adsorption–desorption process are finite, Eq. (9) is solved with the appropriate kinetic model:

$$\frac{\partial q_i}{\partial t} = g(\mathbf{C}, \mathbf{q}) \tag{16}$$

Eqs. (9) and (16) constitute the reaction-dispersive model.

2.2.1. The OCFE method

The method of solving differential equations using orthogonal collocation (OC), introduced by Villadsen and Michelsen [8] and regarded as one of the most accurate, was successfully applied in modelling chemical engineering processes. In the case of HPLC, a modified version of OC on finite elements is used in a number of works, e.g., Refs. [9,10]. OC was also applied and successfully implemented in a moving finite elements version for modelling multicomponent fixed-bed adsorption and chromatography [11,12].

Although the technique of orthogonal collocation on finite elements is well known, we briefly describe it. Further details can be found in Ref. [11].

2.2.1.1. The OCFE method technique

The technique of orthogonal collocation on fixed finite elements involves the division of space coordinate x into the NS subdomain whose boundaries fulfil the inequalities

$$0 = S_0 < S_1 < \ldots .. < S_{\mathrm{NS}-1} < S_{\mathrm{NS}} = L \tag{17}$$

At any given time the solution is approximated in each k subdomain $(S_{k-1}-S_k)$ by a suitable polynomial function $C^k(\rho^k, t)$, where ρ^k is a local space variable in subdomain k, $k=1,..,\mathrm{NS}$.

The width of the subdomain is:

$$\Delta_k = S_k - S_{k-1} \tag{18}$$

and the space variable ρ^k is defined as follows:

$$\rho^k = \frac{x - S_{k-1}}{\Delta_k};\ \rho^k \in [0, 1] \tag{19}$$

For each subdomain k number $N(k)$ of interior collocation points is chosen as the roots of the Jacobi polynomial $P^{\alpha\beta}_{N(k)}$ [8] with $\alpha=\beta=0$ and the approximate solution is represented in terms of the Lagrange's interpolation formula:

$$C^k(\rho^k, t) = \sum_{j=0}^{N(k)+1} C_j^k(t) * l_j^k(\rho^k) \tag{20}$$

where $l_j^k(\rho^k)$ is Lagrange polynomial of order $N(k)+2$ with the base point $\{0,\rho_1^k,..,\rho_{N(k)}^k, 1\}$ and $C_j^k(t) = C^k(\rho_j^k, t)$ are the $N(k)+2$ unknown time dependent parameters to be evaluated in order to fully define the approximating polynomial $C^k(\rho^k, t)$ in each kth element.

Because the discretization procedure described above must be applied to the unknown fluid phase concentration C_i, $i=1,..,\mathrm{NC}$ for each subdomain $k=1,..,\mathrm{NS}$, we obtain $\mathrm{NC}*\Sigma_{k=1}^{\mathrm{NS}}[N(k)+2]$ unknown parameters. The $\Sigma_{k=1}^{\mathrm{NS}}N(k)$ parameters are calculated by integrating the following system of ordinal differential equations, which enforce the fulfilment of Eqs. (9) or (15) in the internal collocation points within each subdomain:

$$\frac{\partial C_{ij}^k}{\partial t} + \frac{1-\epsilon_t}{\epsilon_t}\frac{\partial q_{ij}^k}{\partial t} = -\frac{u}{\epsilon_t \Delta_k}\sum_{m=0}^{N(k)+1} A_{jm}^k C_{im}^k + D_a\frac{1}{\Delta_k^2}\sum_{m=0}^{N(k)+1} B_{jm}^k C_{im}^k;\ i = 1,..,\mathrm{NC};\ j = 1,..,N(k);\ k = 1,..,\mathrm{NS} \tag{21}$$

$$\frac{\partial C_{ij}^k}{\partial t} + \frac{1-\epsilon_t}{\epsilon_t}\sum_{m=1}^{NC}\frac{\partial q_{ij}^k}{\partial C_{mj}^k}\frac{\partial C_{mj}^k}{\partial t} = -\frac{u}{\epsilon_t \Delta_k} \times \sum_{m=0}^{N(k)+1} A_{jm}^k C_{im}^k + D_a \frac{1}{\Delta_k^2}\sum_{m=0}^{N(k)+1} B_{jm}^k C_m^k;$$

$$i = 1,..,NC;\ j = 1,..,N(k);\ k = 1,..,NS \quad (22)$$

Next NC*NS*2 parameters are obtained from boundary conditions (Eqs. (11) and (12)): for $x=0$, $k=1$:

$$uC_{fi}' - uC_i^1(0) = -D_a\frac{1}{\Delta_1}\sum_{m=0}^{N(1)+1} A_{om}^1 C_{im}^1;$$

$$i = 1,..,NC \quad (23)$$

for $x=S_{NS}$, $k=NS$:

$$\frac{1}{\Delta_{NS}}\sum_{m=0}^{N(NS)+1} A_{N(NS)+1,m}^{NS} C_{im}^{NS} = 0;\ i = 1,..,NC \quad (24)$$

and from continuity of the solution and the first-order space derivative at the boundary between two neighbouring subdomains: for $x=S_k$; $k=1,..,NS-1$

$$C_{i,N(k)+1}^k = C_{i,0}^{k+1};\ i = 1,..,NC \quad (25)$$

and

$$\frac{1}{\Delta_k}\sum_{m=0}^{N(k)+1} A_{N(k)+1,m}^k C_{im}^k = \frac{1}{\Delta_{k+1}}\sum_{m=0}^{N(k+1)+1} A_{0,m}^{k+1} C_{im}^{k+1};$$

$$i = 1,..,NC \quad (26)$$

In Eqs. (21–26) A and B are equal:

$$A_{jm}^k = \left(\frac{\partial l_m^k}{\partial \rho^k}\right)_{\rho=\rho_j} \quad (27)$$

$$B_{jm}^k = \left(\frac{\partial^2 l_m^k}{\partial \rho^{k2}}\right)_{\rho=\rho_j} \quad (28)$$

The set of discretized equations was solved using two different ways: firstly by the following equilibrium method and secondly by the kinetic method.

2.2.1.2. The OCFE solution – equilibrium method

In fact, the equilibrium method is a classical method commonly used. The set of ordinal differential Eq. (22) obtained after discretization of partial differential Eq. (15), together with algebraic Eqs. (23–26) was solved with Adams–Moulton method implemented in VODE procedure [13].

The derivatives $\partial q_i/\partial C_m$ were calculated analytically for explicit isotherms equation and numerically for implicit isotherm equations. In order to determine surface concentration q_i, the set of nonlinear algebraic equation defining implicit isotherm models were solved with the BUNLSI procedure [14].

2.2.1.3. The OCFE solution – kinetic method

We can start defining the kinetic method applied in this work from analysing the equilibrium-dispersive and the reaction-dispersive model with a simple Langmuir isotherm and a second-order Langmuir kinetic equation, respectively.

The equilibrium-dispersive model for single component Langmuir isotherm can be rewritten as follows:

$$\frac{\partial C}{\partial t} + \frac{u}{\epsilon_t\left(1+\frac{1-\epsilon_t}{\epsilon_t}\frac{\partial q}{\partial C}\right)}\frac{\partial C}{\partial x} = D_a\frac{\partial^2 C}{\partial x^2} \quad (30)$$

$$q = f(C) = \frac{q_s^* K^* C}{1 + K^* C} \quad (31)$$

while the reaction-dispersive is in the form:

$$\frac{\partial C}{\partial t} + \frac{1-\epsilon_t}{\epsilon_t}\frac{\partial q}{\partial t} + \frac{u}{\epsilon_t}\frac{\partial C}{\partial x} = D_a\frac{\partial^2 C}{\partial x^2} \quad (32)$$

$$\frac{\partial q}{\partial t} = g(C,q) = k_a^* C^*(q_s - q) - k_d^* q \quad (33)$$

or using the equilibrium isotherm Eq. (31):

$$\frac{\partial q}{\partial t} = k_d^*\left(\frac{q_s^* K^* C}{1+K^* C} - q\right)^*(1+K^* C) = k_d^*(f(C) - q)^*(1+K^* C) \quad (34)$$

where: k_d and k_a are the rate constants of desorption and adsorption.

From the mathematical point of view, solutions of the models expressed by Eqs. (30) and (31) and (32) and (34) are equivalent when k_d is infinitely high. However, both models coincide for finite, a relatively low value of k_d equals about several tens for overload conditions or low efficiency column. Moreover, if k_d is sufficiently high, the last term in Eq. (34) equal to $(1+K^*C)$ has no influence on calculation results.

It suggests that the solution of the equilibrium-dispersive model with any implicit adsorption isotherm (Eq. (13a)), rewritten as $q_i = f(\mathbf{C},\mathbf{q})$, can be approximated by solution of the model similar to reaction-dispersive one composed of Eqs. (9) and (16a):

$$\frac{\partial q_i}{\partial t} = p^*\left[f(\mathbf{C},\mathbf{q}) - q_i \right] \tag{16a}$$

with sufficiently high value of parameter p. Note, that however parameter p has dimension $(1/s)$, it has not generally a physical meaning.

In the following we call the proposed method the kinetic method.

After discretization due to the OCFE method, the set of partial differential Eq. (9) is reduced to the set of ordinal differential Eq. (21) while the set of Eq. (16a) to:

$$\frac{\partial q_{ij}^k}{\partial t} = p^*\left[f(C_{1j}^k,\ldots C_{\mathrm{NC}j}^k, q_{1j}^k,\ldots,q_{\mathrm{NC}j}^k) - q_{ij}^k \right];$$
$$i = 1,\ldots NC;\ j = 1,\ldots,N(k);\ k = 1,\ldots NS \tag{36}$$

Eqs. (21) and (36) and (23–26) were solved using the VODE procedure.

Note, that in case of kinetic method – Eqs. (21) and (36) – the time consuming, numerical solving of nonlinear algebraic equations due to implicit isotherm equation is avoided.

2.2.2. Finite difference method

The kinetic method described in Section 2.2.1.3 was also implemented for the FD method. The FD method is less robust than the OCFE one but in case of isotherm accounting for surface heterogeneity can be several times faster. Besides, it involves very simple integration algorithm.

In order to solve Eqs. (9) and (16a) the well known forward–backward finite difference scheme was applied:

$$\frac{C_{i,j}^{n+1} - C_{i,j}^n}{\Delta t} + \frac{u}{\epsilon_t}\frac{C_{i,j}^n - C_{i,j-1}^n}{\Delta x} + \frac{1-\epsilon_t}{\epsilon_t} * p^*$$
$$\times\left[f(C_{1,j}^n,\ldots,C_{\mathrm{NC},j}^n, q_{1,j}^n,\ldots,q_{\mathrm{NC},j}^n) - q_{i,j}^n \right] = 0;$$
$$i = 1,..,\mathrm{NC} \tag{37}$$

$$\frac{q_{i,j}^{n+1} - q_{i,j}^n}{\Delta t}$$
$$= p^*\left[f(C_{1,j}^n,\ldots,C_{\mathrm{NC},j}^n, q_{1,j}^n,\ldots,q_{\mathrm{NC},j}^n) - q_{i,j}^n \right];$$
$$i = 1,..,\mathrm{NC} \tag{38}$$

where j is the index of the nodal point and n is the index of the time interval.

In the finite difference approximation of Eq. (9) the dispersion term is usually ignored. The effect of band broadening due to dispersion is approximated by appropriate choosing of space and time increments [6]. Moreover, time increment should fulfil stability conditions. In monograph [6] the stability conditions for different finite difference schemes in linear chromatography were formulated, however, numerical stability conditions for finite difference scheme (Eqs. (37) and (38)) is unknown.

In this work, for calculation of the space interval a typical condition, Δx = height equivalent to a theoretical plate (HEPT), was applied [6]. The time interval Δt was calculated from following relationship:

$$\Delta t = \frac{1}{p^* b} \tag{39}$$

with $b \geq 3$, stability of the differential scheme (Eqs. (37) and (38)) was achieved in any investigated bellow case. Thus, in the following $b = 3$ was applied for all simulations under discussion.

Generally the value of parameter b should be established with the trial and error method.

3. Validation and comparison of the methods proposed

In all the following simulations the process conditions were assumed as: column length $L = 0.1$ m, total porosity $\epsilon_t = 0.8$, mobile phase velocity (superficial velocity) $u = 0.0012$ m/s. Value of isotherm parameters, according to Ref. [4], are presented in Table 1.

In the case of the OCFE method the number of internal collocation points inside subdomain was equal 3. Number of subdomain NS was equal NS = 10, 50, 200 and 600 for number of theoretical plates equal $N = 100$, 500, 3000 and 10 000, correspondingly.

The calculations were performed on Pentium II 350 MHz personal computer.

Both method OCFE and FD preserve the mass balance well. In our calculations the relative error of mass balance fulfilment was less than about 0.1%.

3.1. Validation of kinetic method – OCFE solution

To validate the kinetic method we compared solutions of Model (9), coupled with the Langmuir competitive isotherm, using equilibrium and kinetic methods.

In Figs. 1–3 the comparison of simulations of the band profiles for linear chromatography (loading factor equal 0.084%) and strong overload conditions (loading factor equal 50%) is presented. Times of calculations are given in Table 2.

As can be seen, for the low performance column or strong overload conditions differences between solutions are negligible for parameter p greater than about 10. At $p=50$, the equilibrium and kinetic methods give practically the same results. For high-performance linear chromatography and a low value of loading factor, equivalence between solutions is achieved for higher value of parameter p, e.g., when $N=3000$, p should be equal 2000.

It is possible to arbitrarily choose a very high p value to be sure that it is appropriate for all process conditions, however the time of calculation increases with increasing p value. Thus, if simulations are supposed to be repeated many times it is more convenient to determine an adequate value of parameter p after several trial computations.

In Figs. 4 and 5 the comparison of the equilibrium and kinetic methods for FG isotherm is presented. The loading factor is equal to 6%. Calculation times are given in Table 2. The peak profiles obtained with both methods coincide for parameter p greater than about 100. In this case, time of calculation with the equilibrium method is remarkably longer compared to the kinetic one. Rapid increase of computation time with the use of the equilibrium method for the FG isotherm is a consequence of necessity of solving implicit isotherm equations in order to calculate adsorbed phase concentration q_i.

Because of the very long CPU time the equilibrium method discussed cannot be used for solving more complex implicit isotherms including surface

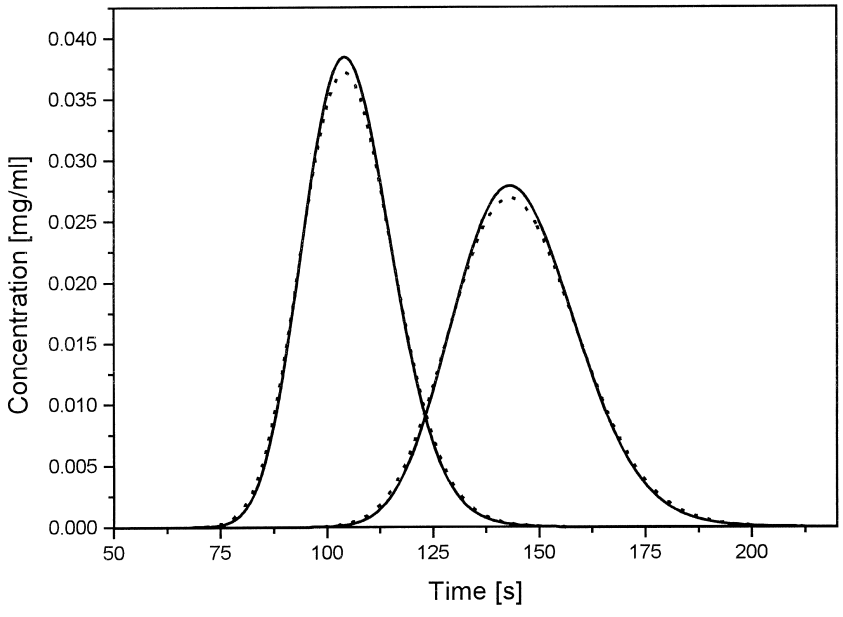

Fig. 1. Comparison of simulations of the band profiles with Langmuir competitive isotherm. Solid lines: solution using equilibrium method. Dotted lines: solutions using kinetic method for coefficient $p=10$. For $p=50$ solution of both methods are undistinguished. The inlet concentration: $C_1=C_2=1$ mg/ml, injection time=1 s, $N=100$.

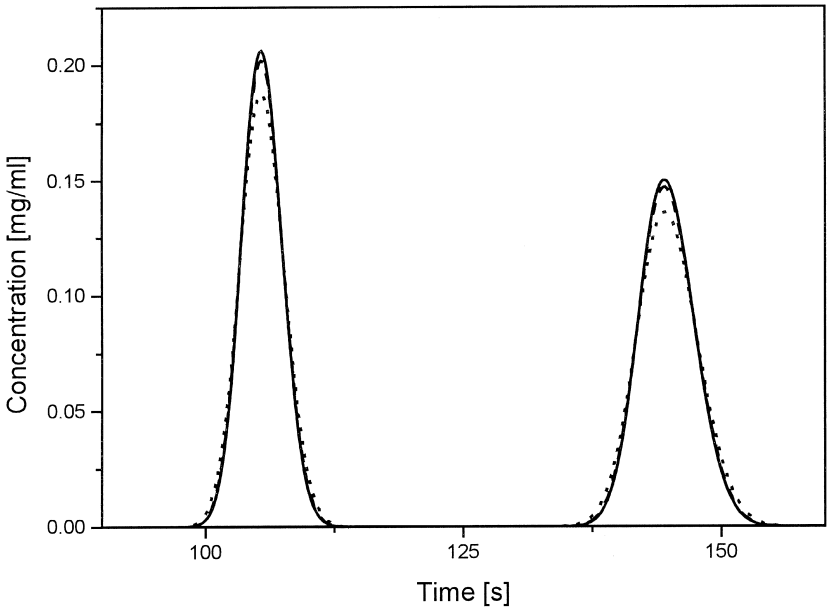

Fig. 2. Comparison of simulations of the band profiles with Langmuir competitive isotherm. Solid lines: solution using equilibrium method. Dotted lines: solutions using kinetic method for coefficient $p=100$, dashed $p=500$. For $p=2000$ solution of both methods are undistinguished. The inlet concentration: $C_1=C_2=1$ mg/ml, injection time=1 s, $N=3000$.

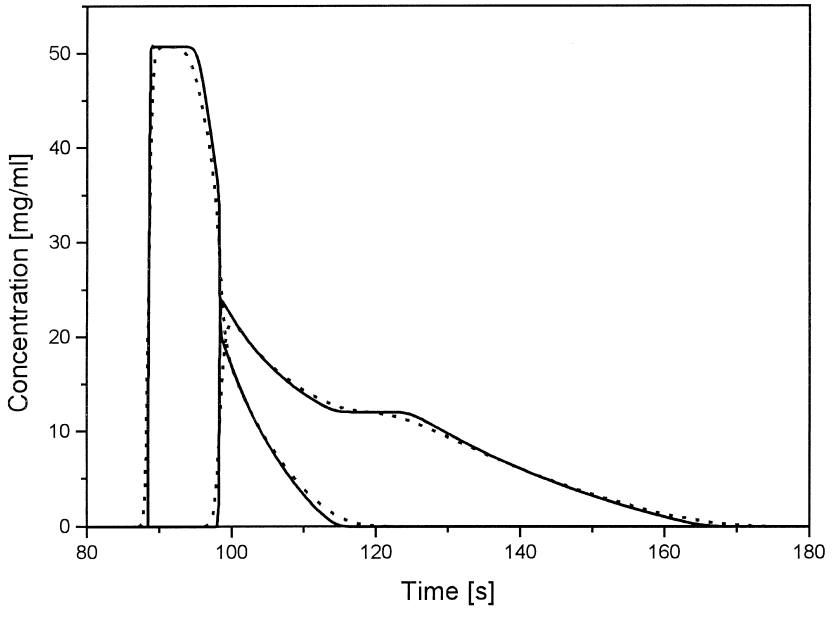

Fig. 3. Comparison of simulations of the band profiles with Langmuir competitive isotherm. Solid lines: solution using equilibrium method. Dotted lines: solutions using kinetic method for coefficient $p=10$. For $p=50$ solution of both methods are undistinguished. The inlet concentration: $C_1=C_2=30$ mg/ml, injection time=20 s, $N=10\,000$.

Table 2
Comparison of CPU times for tested methods: equilibrium method (EM), kinetic method (KM), finite difference method FD

Langmuir isotherm

Feed concentration $C_1=C_2=1$ mg/ml, injection time=1 s				Feed concentration $C_1=C_2=30$ mg/ml, injection time=20 s			
N	EM	KM		N	EM	KM	
	t	p (1/s)	t		t	p (1/s)	t
100	2 s	10	8 s	100	2 s	10	11 s
		50	34 s			50	37 s
500	12 s	10	29 s	500	18 s	10	29 s
		50	2 min 15 s			50	2 min 9 s
		100	4 min 41 s	3000	7 min 57 s	10	4 min 41 s
3000	7 m 43 s	100	19 min 22 s			50	15 min 33 s
		500	3 h 49 min	10 000	23 min 58 s	10	26 min 18 s
		2000	6 h 24 min			50	30 min 33 s

FG isotherm					FG/JF isotherm			
N	EM	p (1/s)	KM	FD	N	p (1/s)	KM	FD
	t		t	t			t	t
100	2 min 10 s	10	10 s	–	100	10	52 s	–
		50	51 s	–		50	4 min	–
		100	1 min 23 s	29 s		100	7 min 20 s	53 s
500	9 min 58 s	10	42 s	–	500	10	3 min 23 s	–
		50	3 min 3 s	–		50	12 min 37 s	–
		100	5 min 54 s	2 min 23 s		100	24 min 31 s	4 min 20 s
3000	1 h 25 min 10 s	10	2 min 29 s	–	3000	10	13 min 28 s	–
		50	10 min 42 s	–		50	1 h 27 min	–
		100	21 min 18 s	14 min		100	3 h 15 min	26 min 57 s

heterogeneity parameter. In our numerical test with the equilibrium method for FG/JF or FG/FL isotherms the calculations have been interrupted after 24 h without getting peak profiles.

3.2. Comparison of the OCFE and FD methods

The time of calculation with the OCFE method, especially for implicit isotherm accounting surface heterogeneity such FG/JF and FG/FL, is relatively long – see Table 2. CPU time can be reduced from two-fold (FG isotherm) to about six-times (FG/JF and FG/FL isotherms) when the FD method proposed above is applied. The simulations performed with OCFE and FD give the undistinguished results – see Figs. 6 and 7.

4. Simulations for the selected isotherms

As mentioned before, solutions obtained with the kinetic and the equilibrium methods are fully equivalent, provided the parameter p ranges from 50 to 100 (except for linear chromatography; see Section 3.1). Further increase of the p value exerts no perceptible impact on the band shapes for any isotherm model investigated in this paper. In the simulation discussed we assumed $p=100$ and the number of theoretical plates as equal to 3000. Calculations were performed with aid of the OCFE and FD methods. With both methods, the obtained peak profiles were exactly the same.

The results of simulations of the elution band profiles, obtained for the isotherm models exhibiting the highest Fisher parameter (i.e., for FG/LF, Eqs.

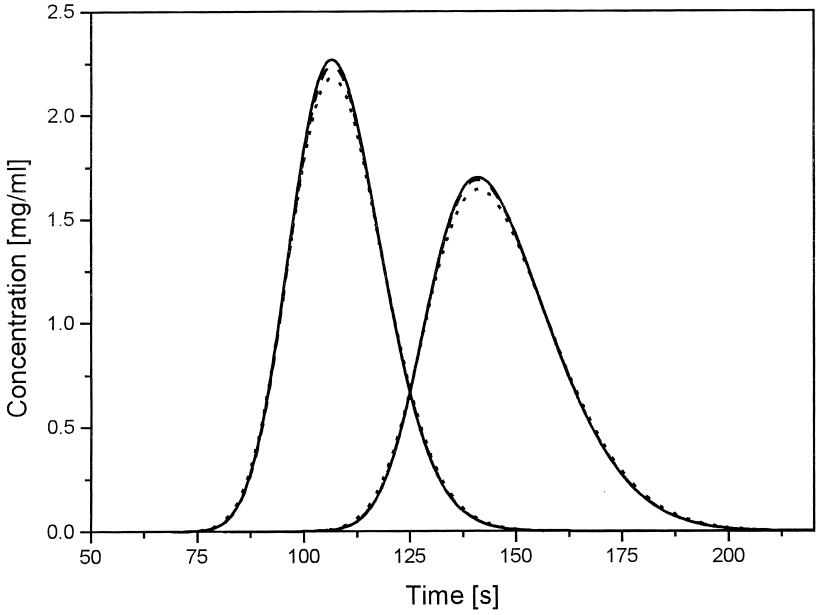

Fig. 4. Comparison of simulations of the band profiles with FG isotherm. Solid lines: solution using equilibrium method. Dotted lines: solutions using kinetic method for coefficient $p=10$, dashed lines $p=50$. For $p=100$ solution of both methods are undistinguished. The inlet concentration: $C_1=C_2=6$ mg/ml, injection time=10 s, $N=100$.

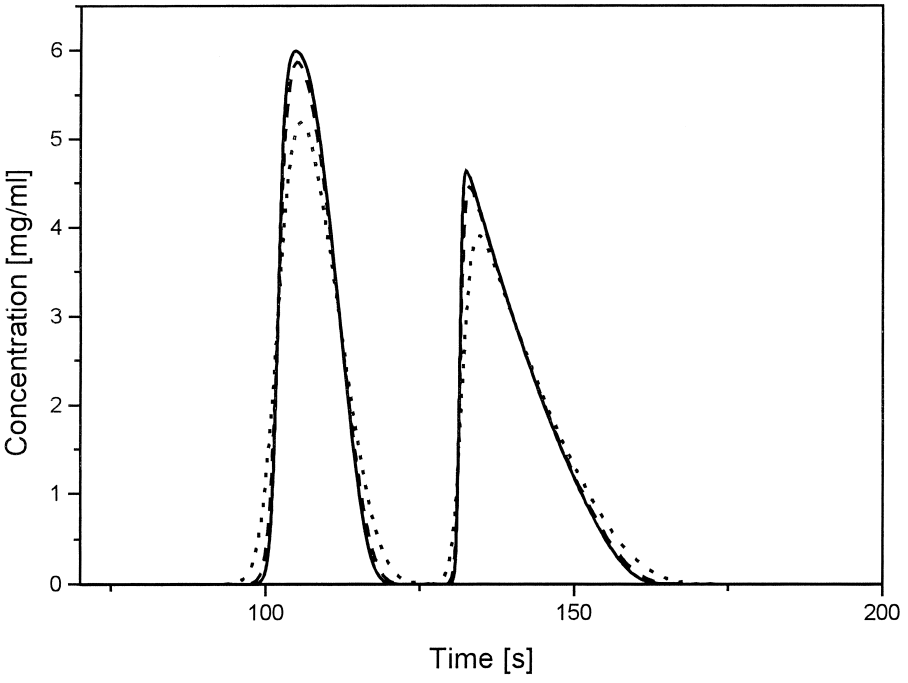

Fig. 5. The same as Fig. 4, but $N=3000$.

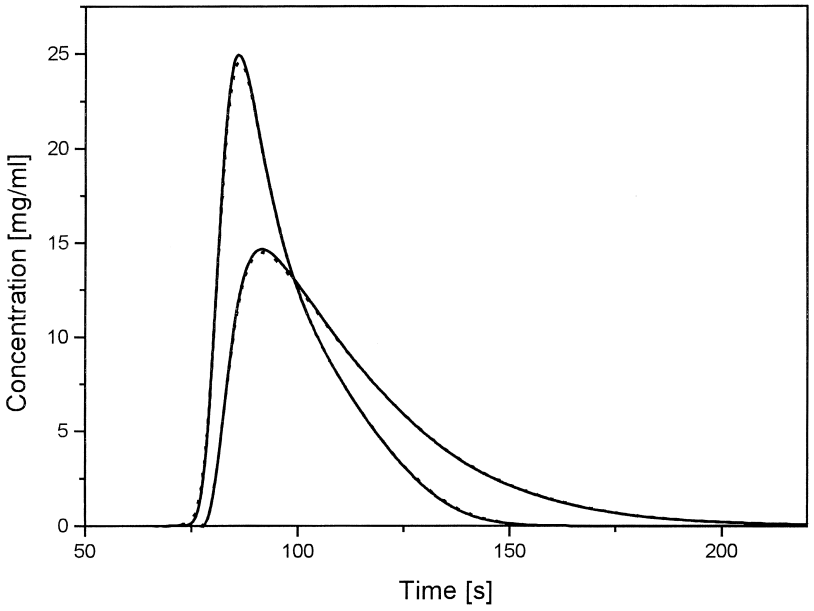

Fig. 6. Comparison of simulations of the band profiles with FG/JF isotherm using OCFE and FD kinetic method. Dotted lines: coefficient $p=10$, solid lines $p=50$ and $p=100$. The inlet concentration: $C_1=C_2=30$ mg/ml, injection time=20 s, $N=100$.

(1) and (2), and for FG/JF, Eqs. (3) and (4) are valid, see also Table 1), are presented in Figs. 8 and 9.

The results of calculations with use of the both isotherm models are similar to one another. Because of the relatively high surface heterogeneity predicted

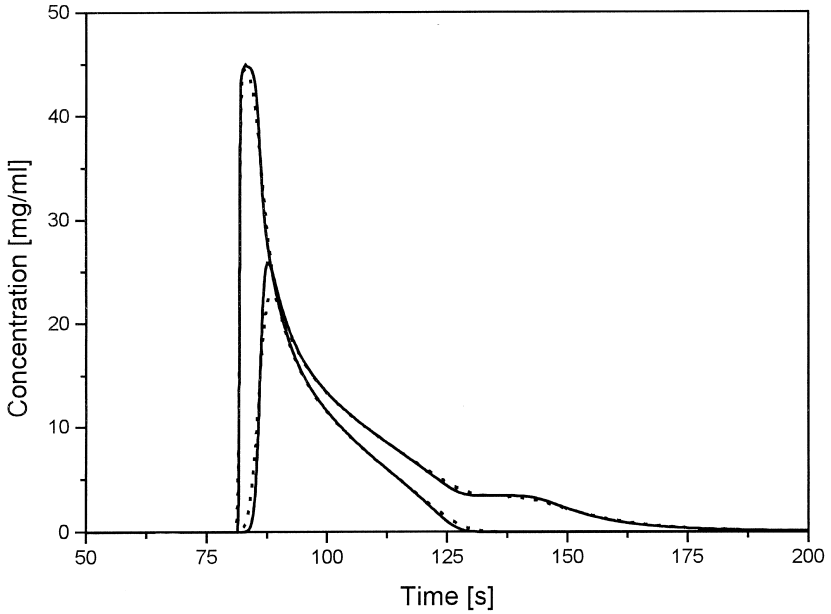

Fig. 7. The same as Fig. 6, but $N=3000$.

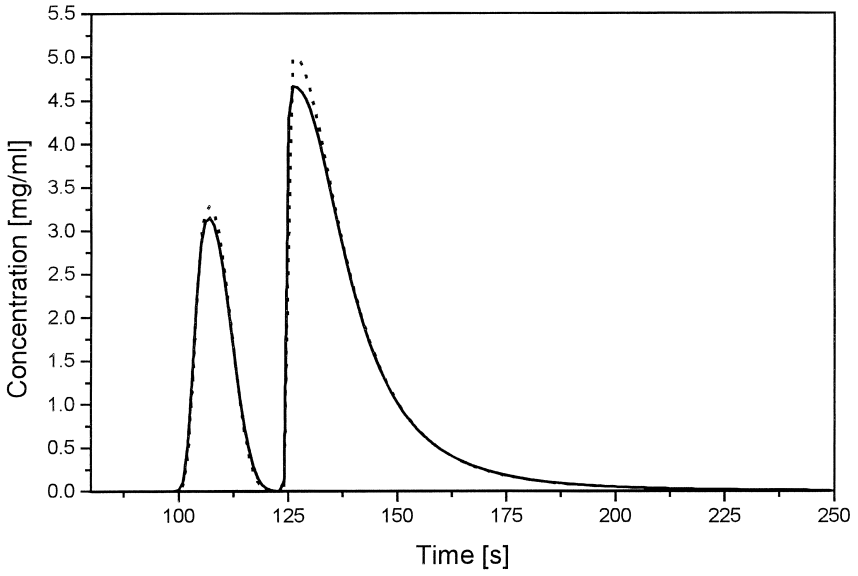

Fig. 8. Comparison of the band profile predicted with FG/LF (solid) and FG/JF (dotted). Feed concentrations ratio: 1:3, total mobile phase concentration: 12 mg/ml, injection time: 10 s.

for the second component (see Table 1), the peak profile of this component exhibits a strong tailing. Such phenomena appear in the case of very low sample concentrations also (as shown in Fig. 10, where simulations with the FG/JF isotherm for the feed concentrations $C_1 = C_2 = 1$ and $C_1 = C_2 = 0.1$ mg/ml are presented). Moreover, a significant shift of the retention time can be observed with the decreasing feed concentration of the second component. These phenomena result from the very nature

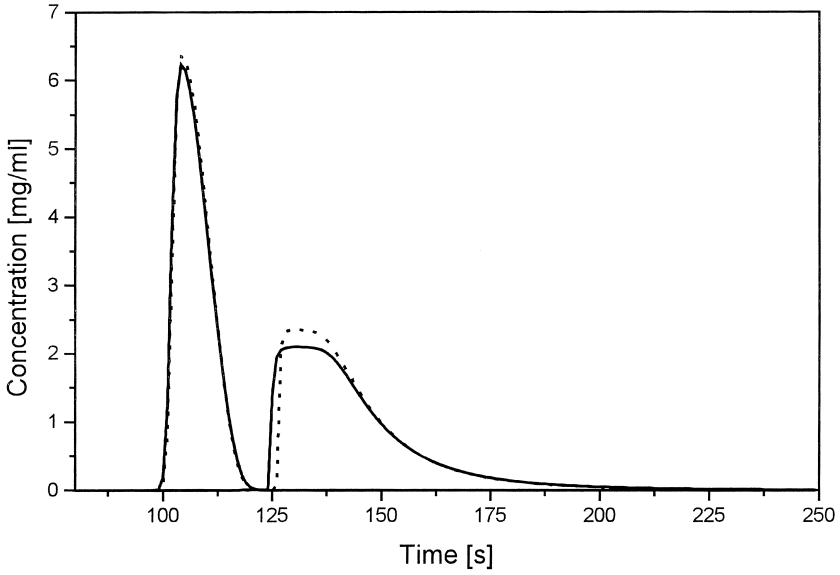

Fig. 9. Similar to Fig. 8, but feed concentrations ratio: 1:1.

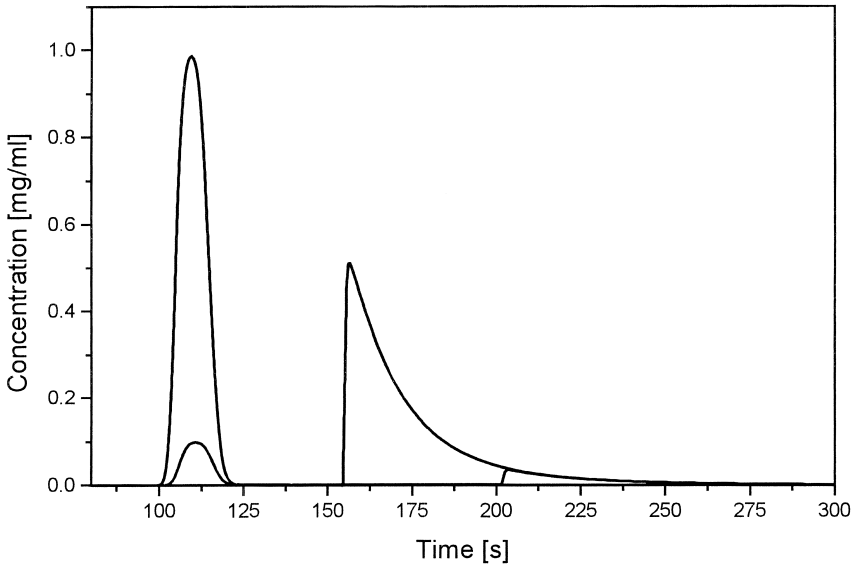

Fig. 10. Prediction of the band profile with FG/JF model. Feed concentrations $C_1 = C_2 = 1$ and $C_1 = C_2 = 0.1$, injection time: 10 s.

of the heterogeneous model, in which the derivatives $\partial q/\partial C$ describing retention time of the components tend to infinity for the infinitely low feed concentration, i.e., $\left.\frac{\partial q}{\partial C}\right|_{C\to 0} \to \infty$. The greater the surface heterogeneity, the more pronounced the described phenomenon. In spite of a very low concentration, which suggests the linear range of the common isotherms, the Gaussian peak profile was not recorded.

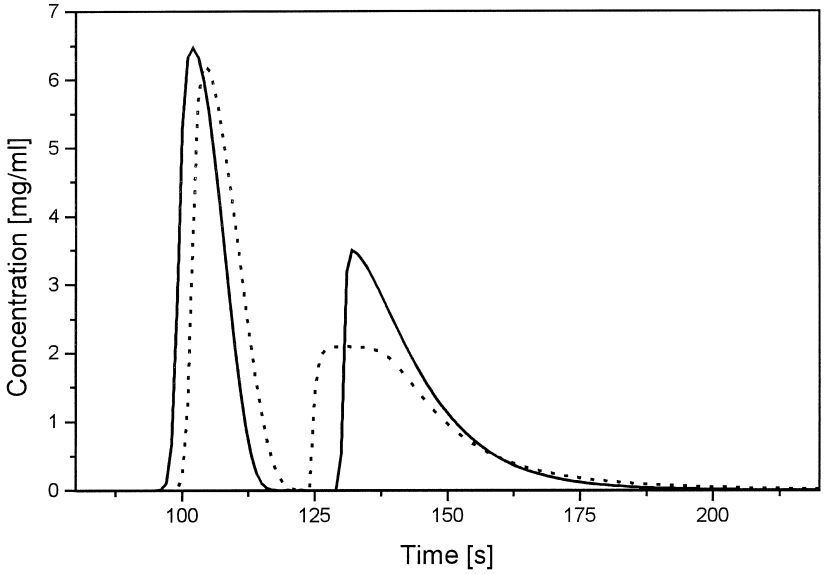

Fig. 11. Comparison of the band profile prediction with JF model (solid) and FG/LF (dotted). Feed conditions as in Fig. 8, but concentration ratio = 1:1.

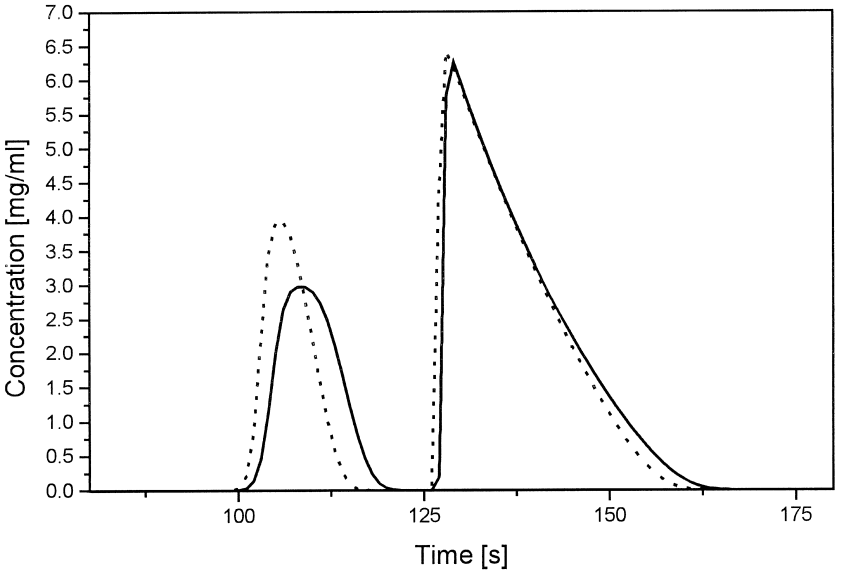

Fig. 12. The comparison of the band profile prediction with FG model (solid) and Langmuir competitive isotherm model (dotted). Feed conditions as in Fig. 8.

Similar behaviour is predicted by the Jovanovic–Freundlich model (Eqs. (5) and (6)), devised for the cases of surface heterogeneity and characterised by a relatively high Fisher parameter (see Table 1). As the heterogeneity predicted by this model is lower than that predicted by the FG/LF and FG/JF models, the observed peak tailing is less considerable (see Fig. 11). Distance between the band profiles of the two

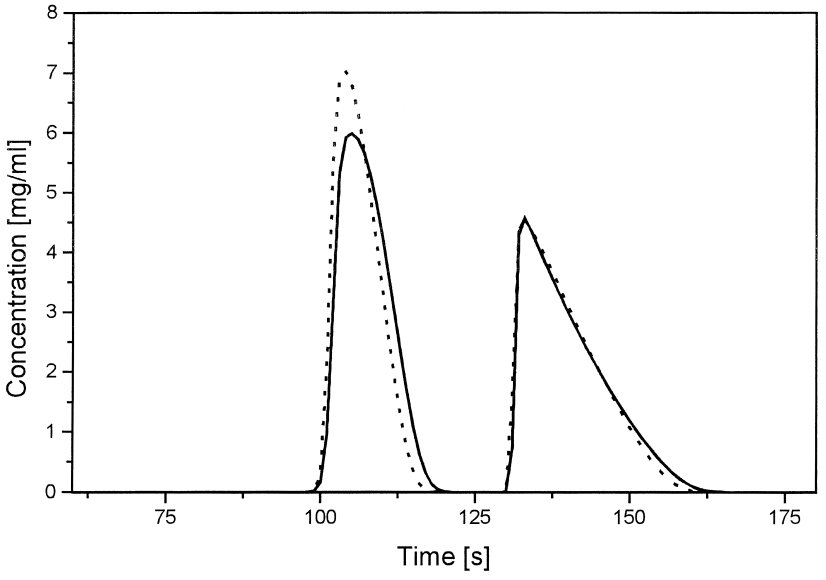

Fig. 13. The comparison of of the band profile prediction with FG model (solid) and Langmuir competitive isotherm model (dotted). Feed conditions as in Fig. 8, but concentration ratio = 1:1.

components simulated with aid of the JF model increases as a result of neglecting the attractive adsorbate–adsorbate interactions.

The aforementioned significant growth of the retention time with the decreasing concentration of the second component disappears for the isotherm models neglecting surface heterogeneity (such as, e.g., the FG model). In Figs. 12 and 13, the results of the band profile simulation with use of the FG model are compared with those resulting from the simple Langmuir competitive model. Differences between simulations for the first component are caused by the attractive lateral interactions, recognised within the framework of the FG model.

5. Conclusion

The numerical kinetic method for solving mathematical model of chromatography process coupled with implicit isotherm models has been proposed. The method was implemented in orthogonal collocation and finite difference forward–backward algorithm. The accuracy of method was compared with the classical equilibrium method.

The equilibrium method has proved to be not robust, the calculation times were always remarkably greater in comparison with the kinetic method. Moreover, for isotherms accounted surface heterogeneity computation time was prohibitively long.

The kinetic method, derived from the kinetic model, was successfully examined for five different isotherms, low- and high-performance columns in analytical as well as overload conditions. Calculation time with the kinetic method combined with finite difference algorithm was relatively low and was equal for the most sophisticated FG/JF and FG/FL isotherms about 1 min at 100 theoretical plates and 30 min at 3000 theoretical plates.

The kinetic method is supposed to enable simulation of chromatography column processes for any implicit isotherm. It can be also easily implemented in more complex chromatography models.

6. List of symbols

- a, isotherm parameter
- b, parameter introduced in Eq. (39)
- C, $\mathbf{C}$, component concentration or vector of components concentration in bulk phase, respectively
- D_a, apparent dispersion coefficient
- F, Fisher parameter
- k, subdomain index
- K, equilibrium constant
- k_d, k_a, rate constants of desorption and adsorption, respectively
- l, Lagrange polynomial or number of adjusted parameters
- L, column length
- n, number of data points
- N, number theoretical plates
- $N(k)$, number of interior collocation points in k subdomain
- NC, number of components
- NS, number of subdomains
- p, parameter introduced in Eq. (16a)
- $P_{N(k)}^{\alpha\beta}$, Jacobi polynomial
- q, $\mathbf{q}$, adsorbed phase concentration or vector of adsorbed phase concentrations, respectively
- q_s, total coverage
- S_i, ith boundary of subdomain
- t, time
- t_p, time during the constant concentration is fed into column
- u, superficial velocity
- x, axial coordinate

6.1. Greek letters

- χ, energy of lateral interaction between molecules
- ϵ_t, total porosity
- ν, heterogeneity parameter
- $\theta_i = q_i/q_{is}$, fractional coverage of ith component
- ρ, local space variable
- Δ, width of the subdomain
- Δt, time interval
- Δx, space interval

6.2. Subscripts

- calc, calculated value
- exp, experimental value
- f, inlet value
- i, component index
- j, index of nodal point
- k, subdomain index

6.3. Superscripts

- *k*, subdomain index
- *n*, index of time interval

References

[1] B.P. Russel, M.D. LeVan, Chem. Eng. Sci. 51 (1996) 4025.
[2] I. Quinones, G. Guiochon, J. Colloid Interface Sci. 183 (1996) 57.
[3] M. Jaroniec, R. Madey, Physical Adsorption on Heterogeneous Solids, Elsevier, Amsterdam, 1998.
[4] I. Quinones, G. Guiochon, J. Chromatogr. A 796 (1998) 15.
[5] J. Zhu, A.M. Katti, G. Guiochon, J. Chromatogr. 552 (1991) 71.
[6] G. Guiochon, S. Golshan Shirazi, A.M. Katti, Fundamentals of Preparative and Nonlinear Chromatography, Academic Press, Boston, MA, 1994.
[7] I. Quinones, G. Guiochon, J. Chromatogr. A 734 (1996) 83.
[8] V.J. Villadsen, M.L. Michelsen, Solution of Differential Equation Model by Polynomial Approximation, Prentice-Hall, Englewood Cliffs, NJ, 1978.
[9] Z. Ma, G. Guiochon, Comput. Chem. Eng. 13 (1991) 415.
[10] A.J. Berninger, R.D. Whitley, X. Zhang, N.H.L. Wang, Comput. Chem. Eng. 15 (1991) 749.
[11] K. Kaczmarski, M. Mazzotti, G. Storti, M. Morbidelli, Comput. Chem. Eng. 21 (1997) 641.
[12] K. Kaczmarski, Comput. Chem. Eng. 20 (1996) 49.
[13] P.N. Brown, A.C. Hindmarsh, G.D. Byrne, Variable-Coefficient Ordinary Differential Equation Solver – procedure available in http://www.netlib.org
[14] G.B. Ferraris, E. Tronconi, Comput. Chem. Eng. 10 (1986) 129.